ISSN 1674-1056
http://cpb.iphy.ac.cn
http://iopscience.iop.org/cpb
中国物理 B
Chinese Physics
中国物理
Chinese Physics B

Electrocaloric effect and pyroelectric properties of organic-inorganic hybrid $(C_2H_5NH_3)_2CuCl_4$

Yi Liu(刘义)[1,3], Yan-Fen Chang(畅艳芬)[2], Young Sun(孙阳)[2], Jun Shen(沈俊)[3], Li-Qin Yan(闫丽琴)[2], Zun-Ming Lu(卢遵铭)[1]
Citation: Chin. Phys. B . 2019, 28(11): 117701 . **doi:** 10.1088/1674-1056/ab48db
Journal homepage: http://cpb.iphy.ac.cn; http://iopscience.iop.org/cpb

What follows is a list of articles you may be interested in

Effect of an electric field on the electrocaloric response of ferroelectrics

Hongbo Liu(刘宏波)
Chin. Phys. B . 2018, 27(12): 127701 . **doi:** 10.1088/1674-1056/27/12/127701

On the parameters for electrocaloric effect predicted by indirect method

Hong-Bo Liu(刘宏波)
Chin. Phys. B . 2017, 26(11): 117701 . **doi:** 10.1088/1674-1056/26/11/117701

Composition and misfit strain dependence of electrocaloric effect of $Pb_{1-x}Sr_xTiO_3$ thin films

Qiu Jian-Hua, Ding Jian-Ning, Yuan Ning-Yi, Wang Xiu-Qin
Chin. Phys. B . 2013, 22(1): 017701 . **doi:** 10.1088/1674-1056/22/1/017701

Effect of misfit strain on the electrocaloric effect of polydomain epitaxial ferroelectric thin films

Qiu Jian-Hua, Ding Jian-Ning, Yuan Ning-Yi, Wang Xiu-Qin
Chin. Phys. B . 2012, 21(9): 097701 . **doi:** 10.1088/1674-1056/21/9/097701

Electrocaloric effect and pyroelectric properties of organic–inorganic hybrid $(C_2H_5NH_3)_2CuCl_4$*

Yi Liu(刘义)[1,3], Yan-Fen Chang(畅艳芬)[2], Young Sun(孙阳)[2], Jun Shen(沈俊)[3], Li-Qin Yan(闫丽琴)[2,†], and Zun-Ming Lu(卢遵铭)[1,‡]

[1] School of Material Science and Engineering, Hebei University of Technology, Tianjin 300130, China
[2] Beijing National Laboratory for Condensed Matter Physics, Institute of Physics, Chinese Academy of Sciences, Beijing 100190, China
[3] Key Laboratory of Cryogenics, Technical Institute of Physics and Chemistry, Chinese Academy of Sciences, Beijing 100190, China

(Received 25 March 2019; revised manuscript received 9 September 2019; published online 30 October 2019)

The organic–inorganic hybrid $(C_2H_5NH_3)_2CuCl_4$ (EA_2CuCl_4) single crystals are prepared by the solvothermal condition method. The x-ray diffraction, scanning electron microscopy, dielectric permittivity, pyroelectric current, and heat capacity are used to systematically investigate the electrocaloric performances of EA_2CuCl_4. The pyroelectric currents are measured under various voltages, and the electrocaloric effect (ECE) is calculated. Its ECE exhibits an isothermal entropy change of 0.0028 J/kg·K under an electric field of 30 kV/cm associated with a relatively broad temperature span. Further, the maximum pyroelectric coefficient (p) is 4×10^{-3} C/m^2·K and the coefficient β for generating ECE from electric displacement D is 1.068×10^8 J·cm·K^{-1}·C^{-2} at 240 K. Our results indicate that the ECE behavior of organic–inorganic hybrid EA_2CuCl_4 is in accordance with Jona and Shirane's opinion in which the ECE should occur both below and above the Curie temperature T_c.

Keywords: electrocaloric effect, pyroelectric properties, organic–inorganic perovskite

PACS: 77.70.+a, 77.55.–g, 81.07.Pr **DOI:** 10.1088/1674-1056/ab48db

1. Introduction

Applying an electric field to a dielectric material may produce a large change in the material polarization, and the associated entropy changes may be explored for a broad range of applications such as in chip cooling and temperature regulation for sensors and electronic devices.[1] According to the Maxwell relation between the pyroelectric coefficient and the electrocaloric effect (ECE),

$$\left(\frac{\partial S}{\partial E}\right)_T = \left(\frac{\partial P}{\partial T}\right)_E, \tag{1}$$

where S is the entropy, E the electric field, P the polarization, and T the absolute temperature. The direction of externally applied electric filed E determines the direction of polarized field P and produces the ECE that can lead the entropy and temperature to chnage. It can be realized in the materials such as famous ferroelectric (FE) poly (vinylidene fluoride-trifluoroethylene) [P(VDF-TrFE)] copolymer,[2,3] lead containing perovskites and their solid solutions or strain engineered films in which phase transitions give rise to the ordering of lead atoms that are disordered in the cubic phase,[4–8] and lead-free-based ceramics such as $BaTiO_3$–$Bi(Mg_{1/2}Ti_{1/2})O_3$ and $Ba(Hf_xTi_{1-x})O_3$, *etc*.[9,10] Refrigeration based on the ECE approach is more environmentally friendly and hence may also serve as an alternative to the traditional vapor-expansion/compression approach.

To date, in the ECE area, besides searching the ways to improve the properties with high temperature change (ΔT) and extensive entropy variation (ΔS), caloric effects of the already known FE compounds, for new promising materials, and for novel designs of operation of electrocaloric measurements,[11–13] the researchers have also been interested in the understanding of the mechanism behind the ECE which is not yet established,[14] especially to the relation between the FE phase transition temperature (Curie temperature T_c) and the existing temperature zone of prominent ECE. Fatuzzo and Merz claim that the ECE exists only above T_c in ferroelectrics, where the P is finite in application of E.[15] Mitsui, Tatsuzaki, and Nakamura argued that the ECE does not exist above T_c but is measurable below T_c, where the P changes with temperature (T).[16] Jona and Shirane showed that their results are not in accord with the above results and indicated that the effect occurs both above and below T_c.[17] Afterwards Scott pointed out that first-order FE phase transitions can take place in a wide range of temperatures above T_c, at which E can still induce P and the ECE usually reaches a maximum value in this range.[18,19] However, for second-order transitions, the ECE is often nearly non-existent above T_c.[20,21] In this respect, this important issue about the dependence of ΔS and maximum

*Project supported by the Fujian Institute of Innovation, Chinese Academy of Sciences (Grant No. FJCXY18040303), the Youth Innovation Promotion of the Chinese Academy of Sciences (Grant No. 2013004), and the National Natural Science Foundation of China (Grant Nos. 51676198 and 51771067).

†Corresponding author. E-mail: lqyan@iphy.ac.cn
‡Corresponding author. E-mail: luzunming@hebut.edu.cn

© 2019 Chinese Physical Society and IOP Publishing Ltd

entropy $\Delta S_{\max}(E,T)$ on temperature is worthy to be studied experimentally.

Here in this work, we choose the organic–inorganic hybrid $(C_2H_5NH_3)_2CuCl_4$ (EA_2CuCl_4), which belongs to the family of the organic–inorganic hybrid halide perovskite materials, to investigate its pyroelectric and electrocaloric effects. The family of the organic–inorganic hybrid halide perovskite materials has been intensely studied due to photonic, electronic, and potential cooling agent properties.[22–24] The EA_2CuCl_4 exhibits a low-dimensional layered perovskite structure consisting of staggered layers of corner sharing $CuCl_6$ octahedron separated by two layers of ethylammonium group $(C_2H_5NH_3)^+$.[25] It undergoes a series of structural phase transitions due to the Jahn–Teller effect combined with the arrangement orientational order and conformation of the organic molecules of the $(C_2H_5NH_3)^+$ chains.[26,27] It was reported as a multiferroic material with a large P value in FE phase.[25–27] Its FE–PE (paraelectric) transition is continuous with a second-order phase transition around 247 K ascribed to an unchanged space group *Pbca* below 330 K.[26,27] To testify the correlation between ΔS distribution with respect to T and phase transition temperature, in this paper, the fundamental study on ECE in a prototype organic–inorganic hybrid EA_2CuCl_4 is conducted.

2. Experiments

The EA_2CuCl_4 single crystals used in this investigation were prepared by a solvothermal condition method from an aqueous solution, which contained stoichiometrically $C_2H_5NH_2{\cdot}HCl$ and $CuCl_2{\cdot}2H_2O$. The solution was placed in a 100-ml flat beaker then heated at 70 °C in a thermostat for 3 days. Then the beaker was placed at room temperature (RT) for 5 days for crystallizing the solution by the method of slow evaporation. The obtained crystals were yellow square plates in shape, typically 5 mm× 5 mm (*ab* plane) in area and 0.25 mm in thickness. The crystals were stored in Ar protective atmosphere. The x-ray diffraction (XRD) experiment was performed at RT by using a Rigaku Smart Lab diffraction system combined with Cu-$K\alpha$ radiation, $\lambda = 1.54184$ Å. A scanning electron microscopy (SEM, S-3400 N, Hitachi, Japan) was used to investigate the layered morphology along the [100] direction of EA_2CuCl_4. All electrical measurements were carried out in a cryogen-free superconducting magnet system (Oxford Instruments, Teslatron PT) with a homemade probe. Silver epoxy was painted on the crystals. The dielectric permittivity was measured by an Agilent 4980 A inductance capacitance–resistance (LCR) meter. The pyroelectric currents were recorded by a Keithley 6517B electrometer. Before the pyroelectric current measurements, the specimen was prepolarized by the electric field from the 300 K (PE phase) into 200 K (FE phase). After removing the polarized electric field and releasing space charges for 30 min until the background current J was less than 0.02 pA, the pyroelectric currents were then collected with increasing temperature. The electric polarization P was obtained by integrating the pyroelectric currents with respect to time. The heat capacity was measured by using a physical property measurement system (Quantum Design).

3. Results and discussion

Figure 1 and its inset show the powder and single crystalline XRD patterns at RT for EA_2CuCl_4 compound, respectively. Powder XRD pattern has confirmed the structure and phase purity of the obtained sample, revealing the single phase perovskite structure with space group *Pbca* at RT, which is in agreement with the result in the literature.[28] The single-crystal XRD pattern suggests that the crystal is naturally grown along the [100] direction.

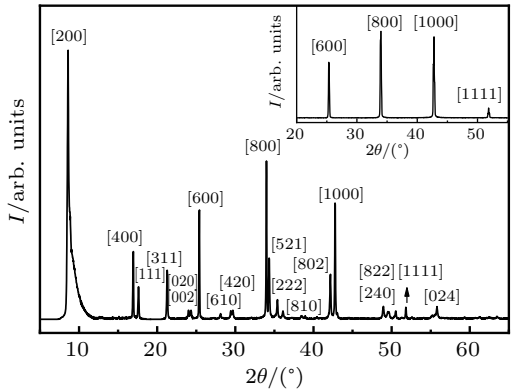


Fig. 1. XRD diffraction patterns of powder EA_2CuCl_4 and single crystalline sample along [100] direction (the inset) at RT.

Figure 2 shows the SEM image of single crystalline EA_2CuCl_4 at RT. It is obviously shown that the layers are well stacked along the a axis. The bc plane is shiny like mirror without visible voids or pores. The crystal quality can also be ascertained by the homogeneous texture.

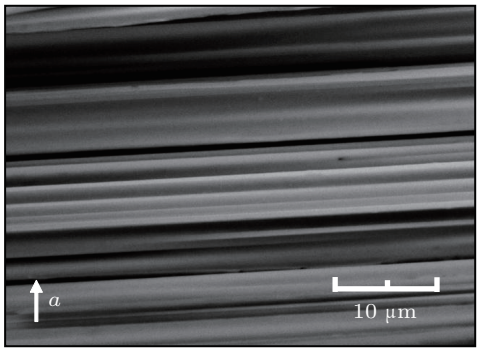


Fig. 2. SEM image of single crystalline EA_2CuCl_4 at RT.

The dielectric permittivity (ε) and its loss tangent ($\tan\delta$) along the [100] direction of the EA_2CuCl_4 crystal as a function of temperature in a frequency range of 1 kHz–1 MHz are

shown in Fig. 3 and its inset, respectively. One can see that the increasing of frequency can reduce both ε and $\tan\delta$. During heating the crystal, an anomaly in the temperature region of 220 K–275 K appears, *i.e.*, an abrupt peak at 250 K. It reveals a transition from PE to improper FE phase at $T_c = 250$ K, as evidenced by the sudden jump and the broad shape above T_c in the ε–T and $\tan\delta$–T curves. The sudden jump at T_c suggests an FE phase transition induced by an order–disorder transition of hydrogen bonds as a common feature in $(C_nH_{2n+1}NH_3)_2MCl_4$ perovskites.[25,29] It may relate to the reorientation of the organic chains among four equivalent orientations inside the cavity of the $CuCl_6$ octahedron.[30,31] By the way, the phase transition temperature T_c of this film refers to the temperature at which electric polarization can occur in the compound. The small difference (3 K) in T_c between our measurements and the reported result of the literature should originate from the technique procedure and environmental factors of sample growth.[25] Here, another distinct characteristic temperature at $T_f = 275$ K can also be observed in the $\tan\delta$–T and corresponding ε–T curve. This temperature can be considered as the final temperature resulting from the FE domain movement or Jahn–Teller effect-related distortion of the compound. Additionally, a wide dip in ε–T and the corresponding hump in $\tan\delta$–T below T_c are also existent as indicated by the symbol "*". It should be mainly related to the incomplete recovery of the ferroelastic domains in the temperature change process.[26]

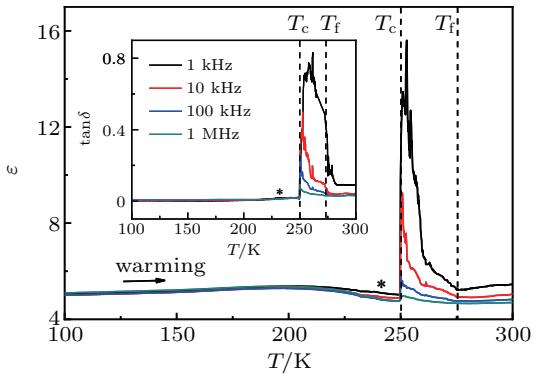


Fig. 3. Dielectric permittivity (ε) and loss tangent ($\tan\delta$) (inset) *versus* temperature, with dashed lines indicating T_c and T_f. Dielectric phase transition is observed at $T_c = 250$ K.

We also measure the pyroelectric current J along the [100] direction in an electric field $\boldsymbol{E}$ range of 8 kV/cm–30 kV/cm as shown in Fig. 4(a). The pyroelectric current exhibits a wide temperature zone dependence in a T range of 220 K–275 K, showing a broad peak shape consistent with the behavior of the temperature dependence of dielectric permittivity (Fig. 3). There are two central peaks at 232 K and 240 K in the curves of J–T, whose direction can be switched oppositely by a negative electric field, revealing an FE order in nature. Two separated maxima at 232 K and 240 K are developed below $T_c = 250$ K (the defined Curie temperature by ε–T measurement). The peak intensity increases with the increase of $\boldsymbol{E}$. After integrating the pyroelectric current density with respect to time, the P *versus* T curves are obtained with different prepolarized electric fields as shown in Fig. 4(b). The polarization P increases systematically with $\boldsymbol{E}$ increasing, and the largest P is 0.084 μC/cm^2 for the highest $\boldsymbol{E} = 30$ kV/cm. The slowly increasing trend of P below 275 K with T decreasing seems to imply a second-order phase transition from PE to FE.

In terms of the previous literature, these two peaks located, respectively, at 232 K and 240 K on J–T curves should arise from different types of structural orderings of the compound.[25–27] The determined temperature at which the material undergoes a second-order phase transition is $T_c = 250$ K according to ε–T measurements. A delayed maximum peak at 240 K in J–T measurements corresponding to the FE phase transition at T_c in ε–T and $\tan\delta$–T curves. It is related to the reorientation of the organic chains among four equivalent orientations inside the cavity of the $CuCl_6$ octahedron.[25,32] The additional transition temperature at 232 K in J–T curve is coupled to the wide dip indicated by symbol "*" in ε–T and $\tan\delta$–T curves which is related to structural change caused by ferroelastic deformation.[25–27]

It is noteworthy that the polarization intensity P is far from saturation due to our limited experimental applied voltage. As the $\boldsymbol{E}$ increases, P should increase rapidly. However, this P value is far lower than the reported 18 μC/cm^2 by Kundys *et al.*[25] We experimentally repeat the pyroelectric current measurements several times, and the J value remains unchanged after using different batches of pieces. As reported in the literature by Kundys *et al.*, their prepolarized electric field $\boldsymbol{E}$ for the P–T measurement is unavailable which might be responsible for the large difference in P.[25]

Pyroelectric current J is measurable and changeable with E until 275 K above T_c. This pyroelectric current behavior is in accordance with that from the Jona and Shirane's viewpoint in which the ECE exists both above and below T_c.[17] However, considering Scott's principle in a phase-transition-type way of ECE, the J–T behavior reflects against the second-order phase transition instead of first-order type since the ECE is maintained till 275 K above T_c. This conclusion on the order type of FE phase transition in EA_2CuCl_4 needs further clarifyingthrough in-depth study of crystal structure.[33]

The pyroelectric coefficient p in different values of E is presented in Fig. 4(c), which is defined by the first derivative of of P with respect to T as shown in the following equation:

$$p = \mathrm{d}P/\mathrm{d}T. \tag{2}$$

The p shows exactly the same T-dependent profile as J: they peak at 232 K and 240 K. The peak value of p reaches 4×10^{-3} C/m^2·K at $\boldsymbol{E} = 30$ kV/cm. This p value is smaller than those reported in organic ferroelectrics[34–36] and some traditional inorganic ferroelectrics.[37–39] It should be ascribed

to the broad temperature span of FE–PM phase transition and the unsaturated P.

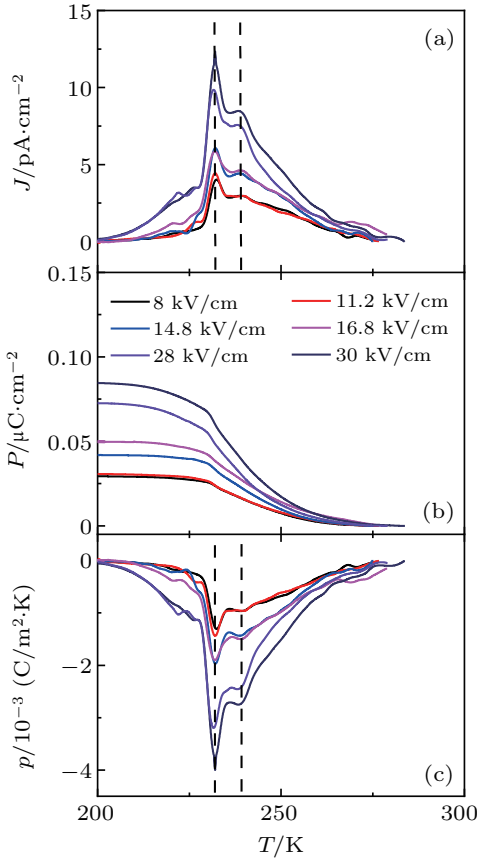


Fig. 4. (a) Plots of pyroelectric current J along [100] *versus* temperature under various prepolarizing electric fields, where dashed lines indicate peak positions. (b) Plots of electric polarization P along [100] *versus* temperature, obtained by integrating the pyroelectric current with respect to time. (c) Plots of pyroelectric coefficient p *versus* temperature, where dashed lines indicate peak positions.

Electrocaloric effect is calculated by an indirect method, and the calculation formula of specific entropy (ΔS) under isothermal condition can be expressed as follows:

$$\Delta S = -\frac{1}{\rho}\int_{E_1}^{E_2}\left(\frac{\partial P}{\partial T}\right)\mathrm{d}E, \tag{3}$$

where ρ, P, and T are the mass density, electric polarization and temperature, respectively; $\boldsymbol{E}_1$ and $\boldsymbol{E}_2$ are the initial and final applied electric field.

Figure 5(a) illustrates the temperature dependence of ΔS at various electric fields, calculated from Eq. (3). The maximum peak values of $\Delta S_{\max}$ are remarkably larger at higher electric fields. At $\boldsymbol{E} = 30$ kV/cm, the $\Delta S_{\max}$ is 0.0028 J/kg·K. The ΔS increases with $\boldsymbol{E}$ increasing due to its being far from saturated P.

We further perform the measurement of the heat capacity in zero field (Fig. 6). An obvious thermal anomaly at 240 K corresponds to the ferroelectric transition as shown in the inset of Fig. 6. The adiabatic temperature change (ΔT) is calculated from the following formula:

$$\Delta T = -\frac{T}{\rho C_p}\int_{E_1}^{E_2}\left(\frac{\partial P}{\partial T}\right)\mathrm{d}E, \tag{4}$$

where ΔT, T, ρ, C_p, and P are the adiabatic temperature change, temperature, mass density, specific heat capacity and polarization (obtained from the P–T curves), respectively; E_1 and E_2 are the initial and final applied electric fields, where E_1 is taken to be 0 and E_2 is taken to be the measure electric field. Figure 5(b) shows the variations of ΔT *versus* temperatures T at various electric fields. The amplitude of ΔT is relatively small originating from the unsaturated polarization P.

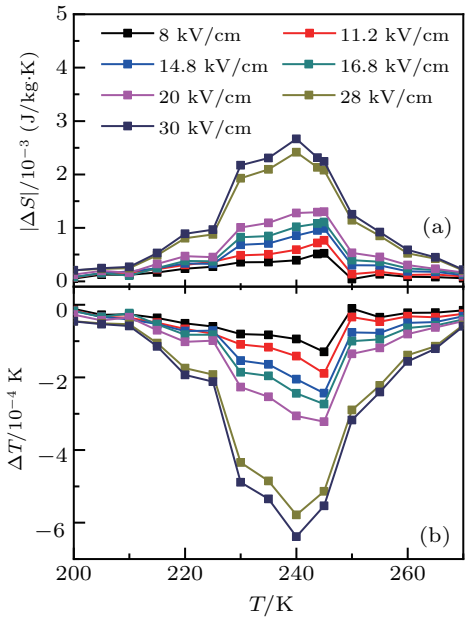


Fig. 5. Plots of (a) $|\Delta S|$ and (b) ΔT *versus* temperature at various electric fields.

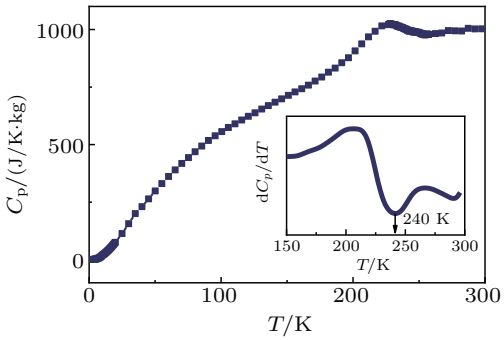


Fig. 6. Plot of heat capacity *versus* temperature at zero field. Inset displays temperature-dependent derivative of heat capacity with respect to temperature.

As organic–inorganic hybrid EA_2CuCl_4 develops a polar phase arising from the arrangement orientational order and configuration of the organic molecules of the $(C_2H_5NH_3)^+$ chains,[25] the entropy change ΔS is proportional to the square of the electric displacement change based on the thermodynamic phenomenological theory,[40,41] and described by the following equation:

$$|\Delta S| = \frac{1}{2}\beta D^2. \tag{5}$$

Thus the coefficient β is regarded as a measure of how effectively a known electric displacement D ($D = \varepsilon_0 E + P$) induces the ECE.

From Fig. 7, we can obtain that $\beta = 1.068 \times 10^8$ J·cm·K^{-1}·C^{-2} at 241 K. In comparison with P(VDF-TrFE) copolymer with 9.3×10^9 J·cm·K^{-1}·C^{-2} and the PLZT thin films with 1.5×10^8 J·cm·K^{-1}·C^{-2}, our result on EA_2CuCl_4 is within a reasonable range.

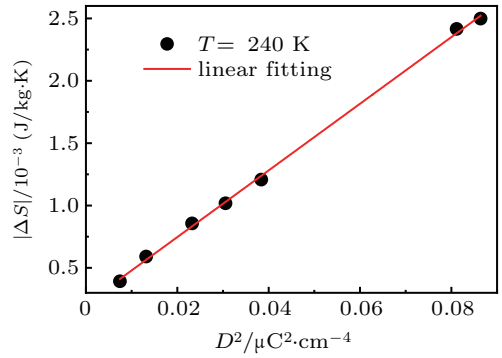


Fig. 7. Relation between ΔS and D^2 at 240 K for EA_2CuCl_4. From slope (solid fitting line) β coefficient is obtained.

From the above measurements and analysis, though the ΔS_{max} are smaller than those from the most conspicuous electrocaloric materials, EA_2CuCl_4 shows a consistent ECE behavior according to the Jona and Shirane's viewpoints. The FE phase transition at $T_c = 250$ K contributes to the ΔS_{max} below T_c, producing ΔS above T_c. However, our results indicate a contradiction between the reported phase transition order type and Scott's mechanism. This issue will be studied in detail in our further work.

4. Conclusions

In this study, EA_2CuCl_4 shows an ECE with a broad temperature span below and above T_c, large coefficient p and β. The obtained results show a consistent ECE behavior with Jona and Shirane's perspective in terms of the ECE existing both below and above FE phase transition temperature in EA_2CuCl_4. The ECE and pyroelectric studies in EA_2CuCl_4 suggest that the family of organic–inorganic hybrids can become a potential multifunctional material with the following merits: (i) low-dimensional crystalline structure, (ii) a wide temperature span of ΔS, and large pyroelectric coefficient p and β, (iii) easy-to-fabricate and easy-to-tune the transition temperature by modifying the organic functional group, and (iv) potentially multicaloric effect.[22]

References

[1] Zhang G, Zhang X, Huang H, Wang J, Li Q, Chen L Q and Wang Q 2016 *Adv. Mater.* **28** 4811
[2] Akcay G, Alpay S P and Mantese J V 2007 *Appl. Phys. Lett.* **90** 252909
[3] Neese B, Chu B, Lu S G, Wang Y, Furman E and Zhang M 2008 *Science* **321** 821
[4] Misirlioglu I B, Alpay S P, Aindow M and Nagarajan V 2006 *Appl. Phys. Lett.* **88** 102906
[5] Zhang J, Alpay S P and Rossetti G A 2011 *Appl. Phys. Lett.* **98** 132907
[6] Mischenko A S, Zhang Q, Scott J F, Whatmore R W and Mathur N D 2006 *Science* **311** 1270
[7] Sternberg A, Birks E, Shebanovs L, Klotins E, Ozolinsh M, Tyunina M, Zauls V and Kundzinsh M 1999 *Ferroelectrics* **226** 217
[8] Olsen R D, Butler W F, Payne D A, Tuttle B A, Held P C 1980 *Phys. Rev. Lett.* **45** 1436
[9] Li M D, Tang X G, Zeng S M, Liu Q X, Jiang Y P and Li W H 2018 *J. Alloys Compd.* **747** 1053
[10] Li M D, Tang X G, Zeng S M, Liu Q X, Jiang Y P, Zhang T F and Li W H 2018 *ACS Sustainable Chem. Eng.* **6** 8920
[11] Correia T and Zhang Q 2014 *Eng. Mater.* **34** 183
[12] Rožič B, Malič B, Uršič H, Holc J, Kosec M, Neese B, Zhang Q M and Kutnjak Z 2010 *Ferroelectrics* **405** 26
[13] Flerov I N, Mikhaleva E A 2008 *Phys. Solid State* **50** 478
[14] Scott J F 2011 *Annu. Rev. Mater. Res.* **41** 229
[15] Fatuzzo E and Merz W J 1967 *Ferroelectricity* (Amsterdam: North-Holland)
[16] Mitsui T, Tatsuzaki I and Nakamura E 1976 *Introduction to the physics of ferroelectricity* (London: Gordon and Breach)
[17] Jona F and Shirane G 1962 *Ferroelectric crystals* (NY: McMillan)
[18] Scott J F 1989 *J. Phys. Soc. Jpn.* **58** 4487
[19] Meyerhofer D 1958 *Phys. Rev.* **112** 413
[20] Li B, Ren W J, Wang X W, Meng H, Liu X G, Wang Z J and Zhang Z D 2010 *Appl. Phys. Lett.* **96** 102903
[21] Li B, Wang J B, Zhong X L, Wang F and Zhou Y C 2010 *J. Appl. Phys.* **107** 014109
[22] Ma Y, Zhai K, Yan L, Chai Y, Shang D and Sun Y 2018 *Chin. Phys. B* **27** 027501
[23] Dong Q, Fang Y, Shao Y, Mulligan P and Qiu J 2015 *Science* **347** 967
[24] Han J, Nishihara S, Inoue K and Kurmoo M 2015 *Inorg. Chem.* **54** 2866
[25] Kundys B, Lappas A, Viret M, Kapustianyk V, Rudyk V, Semak S, Simon C and Bakaimi I 2010 *Phys. Rev. B* **81** 224434
[26] Jahn I R, Knorr K and Ihringer J 1989 *J. Phys.: Condens. Matter* **1** 6005
[27] Kapustianyk V, Rudyk V and Partyka M 2007 *Phys. Status Solidi B* **244** 2151
[28] Steadman J P and Willett R D 1970 *Inorg. Chim. Acta* **4** 367
[29] Kapustianik V, Korchak Yu, Polovinko I, Tchukvinskyi R, Czapla Z and Dacko S 1998 *Phys. Stat. Sol. (b)* **207** 95
[30] Chapuis G, Kind R and Arend H 1976 *Phys. Status Solidi A* **36** 285
[31] Depmeier W, Felsche J and Wildermut G 1977 *J. Solid State Chem.* **21** 57
[32] Kapustianik V, Korchak Yu, Sveleba S, Tchukvinskyi R and Girnyk I 1999 *Acta Phys. Poloica A* **95** 351
[33] Not published
[34] Whatmore R W and Watton R 1986 *Rep. Prog. Phys.* **49** 1335
[35] Ploss B, Shin F G, Chan H L and Choy C 2000 *Appl. Phys. Lett.* **76** 2776
[36] Ploss B, Shin F G, Chan H L and Choy C 2000 *IEEE Trans. Dielectr. Electr. Insul.* **7** 517
[37] Jang H and Jun Y 1997 *Ferroelectrics* **193** 125
[38] Chan W H, Xu Z, Zhai J and Chen H 2005 *Appl. Phys. Lett.* **87** 192904
[39] Zhang H, Chen X, Cao F, Wang G, Dong X, Gu Y and Liu Y 2009 *Appl. Phys. Lett.* **94** 252902
[40] Lu S G, Rožič B, Zhang Q M, Kutnjak Z, Li X, Furman E, Gorny L J, Lin M, Malič B, Kosec M, Blinc R and Pirc R 2010 *Appl. Phys. Lett.* **97** 162904
[41] Lu S G and Zhang Q 2009 *Adv. Mater.* **21** 1983